From Paley Graphs to Deterministic Sensing Matrices with Real-Valued Gramians

Arash Amini, Hamed Bagh-Sheikhi and Farokh Marvasti
Advanced Communications Research Institute (ACRI)
Sharif University of Technology, Tehran, Iran.
Email: aamini@sharif.ir, h_baghsheikhi@ee.sharif.ir, marvasti@sharif.ir

***Abstract*—The performance guarantees in recovery of a sparse vector in a compressed sensing scenario, besides the reconstruction technique, depends on the choice of the sensing matrix. The so-called restricted isometry property (RIP) is one of the well-used tools to determine and compare the performance of various sensing matrices. It is a standard result that random (Gaussian) matrices satisfy RIP with high probability. However, the design of deterministic matrices that satisfy RIP has been a great challenge for many years now. The common design technique is through the coherence value (maximum modulus correlation between the columns). In this paper, based on the Paley graphs, we introduce deterministic matrices of size $\frac{q+1}{2} \times q$ with q a prime power, such that the corresponding Gram matrix is real-valued. We show that the coherence of these matrices are less than twice the Welch bound, which is a lower bound valid for general matrices. It should be mentioned that the introduced matrix differs from the equiangular tight frame (ETF) of size $\frac{q-1}{2} \times q$ arising from the Paley difference set.**

I. Introduction

In general, there are infinitely many solutions to an underdetermined system of linear equations. However, it is nowadays well-known that under certain conditions, the sparsest solution can be unique and one might be able to recover it [1], [2]. Let $\mathbf{x}_{n\times 1}$ be an arbitrary vector from which we have access to the linear samples $\mathbf{y}_{m\times 1} = \mathbf{\Phi}_{m\times n}\,\mathbf{x}_{n\times 1}$, where $m < n$. If $\mathbf{x}_{n\times 1}$ is a k-sparse vector, meaning that $\mathbf{x}_{n\times 1}$ has at most k non-zero elements, and $\mathbf{\Phi}_{m\times n}$ is such that $\mathbf{\Phi x}_1 \neq \mathbf{\Phi x}_2$ for all k-sparse vectors $\mathbf{x}_1 \neq \mathbf{x}_2$, then, $\mathbf{y}_{m\times 1}$ uniquely represents $\mathbf{x}_{n\times 1}$. This property of $\mathbf{\Phi}$ is usually stated with "spark"terminology: the spark of $\mathbf{\Phi}$ is said to be larger than l if any subset of l columns of $\mathbf{\Phi}$ is linearly independent. It is easy to see that unique representation of all k-sparse vectors $\mathbf{x}_{n\times 1}$ via their linear samples $\mathbf{y}_{m\times 1} = \mathbf{\Phi x}$ implies a spark value larger than $2k$ for $\mathbf{\Phi}$, and vice versa [3]. It is interesting to mention that the spark of any Vandermonde matrix $V_{m\times n} = \left[\alpha_i^j\right]_{i,j}$ with distinct α_is is $m+1$.

Although the spark value of $\mathbf{\Phi}$ provides necessary and sufficient conditions for unique representation of sparse vectors $\mathbf{x}$ in terms of $\mathbf{y} = \mathbf{\Phi x}$, it does not guarantee the existence of a computationally feasible method to recover $\mathbf{x}$ from $\mathbf{y}$. Furthermore, it does not establish any bound on the representation error when $\mathbf{x}$ is approximately sparse, or when the samples are contaminated by noise ($\mathbf{y} = \mathbf{\Phi}\,\mathbf{x} + \mathbf{w}$, where $\mathbf{w}$ is a noise vector). The latter drawback is the main reason for avoiding Vandermonde matrices in compressed sensing problems, though they have ideal spark values [4].

The common alternative to spark measure that overcomes the previous shortcomings by imposing stronger constraints on the sensing matrix $\mathbf{\Phi}$ is the restricted isometry property.

Definition 1. *The matrix $\mathbf{\Phi}_{m\times n}$ satisfies RIP of order k with constant $\delta_k \in [0,1)$ if for all k-sparse vectors $\mathbf{x}_{n\times 1}$ we have that*

$$1-\delta_k \leq \frac{\|\mathbf{\Phi x}\|_2^2}{\|\mathbf{x}\|_2^2} \leq 1+\delta_k. \tag{1}$$

A result in [5] shows that the best k-sparse approximation of $\mathbf{x}$ can be stably recovered from $\mathbf{y} = \mathbf{\Phi}\,\mathbf{x} + \mathbf{w}$ by using ℓ_1-minimization techniques, when $\mathbf{\Phi}$ satisfies RIP$(2k, \delta_{2k})$ with $\delta_{2k} < \sqrt{2}-1$. In addition, many families of random $m \times n$ matrices (including Gaussian ensembles) satisfy this property with high probability if $m = \mathcal{O}\big(k\log(\frac{n}{k})\big)$[6].

Unlike the spark measure for which there exists explicit matrices that have ideally large spark values, there is currently no deterministic matrix construction with RIP guarantees that scale similar to random matrices. So far, designing matrices with small "coherence"has been the dominant technique for sensing matrix construction.

Definition 2. *The coherence of $\mathbf{\Phi}_{m\times n}$, denoted by $\mu(\mathbf{\Phi})$, is defined as*

$$\mu(\mathbf{\Phi}) = \max_{\substack{1\leq i,j\leq n \\ i\neq j}} \frac{\left|\langle \boldsymbol{\phi}_i, \boldsymbol{\phi}_j\rangle\right|}{\|\boldsymbol{\phi}_i\|_2\,\|\boldsymbol{\phi}_j\|_2}, \tag{2}$$

where $\boldsymbol{\phi}_i$ stands for the ith column of $\mathbf{\Phi}$.

By using Gershgorin's circle theorem one can show that if $\mathbf{\Phi}$ consists of unit-norm columns, then, it satisfies RIP(k, δ_k) with $\delta_k \leq (k-1)\mu(\mathbf{\Phi})$ whenever $k < 1 + \frac{1}{\mu(\mathbf{\Phi})}$. A trivial consequence is that spark$(\mathbf{\Phi}) \geq 1 + \frac{1}{\mu(\mathbf{\Phi})}$.

One of the early deterministic designs is by DeVore [7]. The construction is based on polynomials over finite fields and the result is a binary matrix with small coherence. Chirp-based matrices were introduced in [8]; the elements of these $m \times m^2$ matrices are complex numbers with magnitude $\frac{1}{\sqrt{m}}$. These matrices are shown to satisfy a weaker form of RIP known as statistical RIP [9]. The connection between error correction codes and sensing matrices has been one of the successful design tools. A bipolar design based on second order Reed-Muller codes is introduced in [10]. In [11], using BCH codes with extremely large minimum distances, bipolar

sensing matrices with small coherence values are constructed. The generalization of binary BCH codes to p-ary codes are applied to introduce complex sensing matrices [12]. The Delsarte-Goethals frames based on Delsarte-Goethals codes are proposed in [13]. The study of ReedSolomon codes to generate complex sensing matrices is presented in [14]. As shown in [15], algebraic curves can be exploited in a similar fashion as in algebraic codes to design binary matrices. Employing the regular structures in finite geometry has been another resource in designing matrices with small coherence [16]. Besides coding techniques, certain submatrices of some unitary matrices such as Fourier matrix are also found to have small coherence values [17]. Instead of strict designs that lead to matrices with small coherence values, one might think of applying numerical minimization to achieve optimal coherence values. One of the advantages of this computationally intensive minimization is the flexibility in the choice of m (number of rows in the sensing matrix) [18]. Note that the following theorem, known as Welch bound, establishes a lower-bound for coherence.

Theorem 1 (Welch bound[19])**.** *The coherence of any [complex-valued] matrix $\mathbf{\Phi}_{m\times n}$ with $n \geq m$ is lower-bounded by*

$$\mu(\mathbf{\Phi}) \geq \sqrt{\frac{n-m}{m(n-1)}}. \tag{3}$$

A matrix that has unit-norm columns and achieves the Welch lower-bound of (3), is referred to as an equiangular tight frame (ETF). ETFs are optimal in the sense of coherence. Unfortunately, they do not exist for all pairs of (m, n), and even the known examples are very limited. A consequence of the Welch bound is that $\mu(\mathbf{\Phi}) \geq \mathcal{O}(\frac{1}{\sqrt{m}})$ for $n \gg m$. Thus, according to coherence-based guarantees we shall have that $m \geq \mathcal{O}(k^2)$, which shows a significant increase in the number of samples m compared to RIP-based guarantees of random matrices. This effect is usually attributed to the shortcomings of coherence-based guarantees. However, a new ETF construction in [20] presents a matrix with optimal coherence value whose spark-based (strongest guarantee) and coherence-based guarantees coincide. The only known matrix construction that breaks the $m \geq \mathcal{O}(k^2)$ barrier is due to Bourgain et al. [21] with $m = \mathcal{O}(k^{2-\epsilon})$, where $\epsilon \approx 10^{-24}$ [22].

In this paper, we construct sensing matrices whose Gramians consist only of non-negative real numbers and achieve coherence values less than twice the Welch lower-bound. The matrices are such that the corresponding Gramians coincide with the adjacency matrix of some Paley graphs except for the main diagonal. We should note that our construction is not the first link between graph theory and compressed sensing: [23] introduces a design based on extractor graphs and some applications of expander graphs are discussed in [24] and [25]. A recent construction based on LDPC codes (related to some bipartite graphs) in [26] is shown to exhibit optimal scaling properties using the null-space property guarantee with high probability. Our construction in this paper, unlike the mentioned graph-based designs, leads to a small coherence value, which is the strongest available type of guarantee.

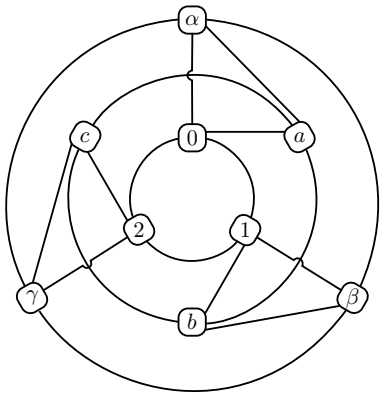

Fig. 1. Paley graph of order $q = 9$. The elements of $\mathbb{F}_9$ are represented by $\{0, 1, 2, a, b, c, \alpha, \beta, \gamma\}$.

II. Paley Graphs

Paley graphs are regular dense graphs associated with quadratic relations in certain finite fields. There are two main distinguishing properties for these graphs:

- they are extremely symmetric, which makes them ideal for mathematical analysis, and
- they are quasi-random, in the sense that they share many properties with random Erdós-Rényi graphs.

Let q be a prime power with residue 1 modulo 4 ($q = 4a+1$ for some integer a) and let $\mathbb{F}_q$ stand for the finite field of size q. If q is a prime, $\mathbb{F}_q$ is simply the integers modulo q. The Paley graph of order q, which we denote by P_q, consists of q vertices, which we will denote by $V_1, V_2, \ldots, V_q$. The edges of the graph are formed by connecting V_i to V_j if and only if $i \neq j$ and $i - j$ has a valid square-root in $\mathbb{F}_q$. The condition $q = 4a + 1$ implies the existence of $\alpha \in \mathbb{F}_q$ such that $\alpha^2 = -1$. Thus, if $i - j$ has a square-root, $j - i$ shall also have one. This confirms that the edges of the Paley graph are well-defined; *i.e.*, V_i is connected to V_j if and only if V_j is connected to V_i. Therefore, the adjacency matrix of P_q, denoted by $A(P_q) = [a_{i,j}]_{q\times q}$ is given by

$$a_{i,j} = \begin{cases} 1 & i \neq j \ \ \& \ \ \exists z \in \mathbb{F}_q,\ i\text{–}j \overset{\mathbb{F}_q}{=} z^2, \\ 0 & \text{otherwise.} \end{cases} \tag{4}$$

For illustration, we have depicted the Paley graph of order $q = 9$ in Figure 1.

As there are $\frac{q-1}{2}$ non-zero squares in $\mathbb{F}_q$, each vertex of the graph is connected to exactly $\frac{q-1}{2}$ vertices. It is also straightforward to see that the graph obtained by shifting the index of vertices is isomorphic to P_q. Hence, the Paley graph enjoys many authomorphisms, which describe its symmetries. In particular, the Paley graphs are members of a larger family known as *strongly regular graphs (srg)*. An $\text{srg}(n, d, n_\lambda, n_\mu)$ is a d-regular graph on n vertices, such that each pair of adjacent

vertices have n_λ commons neighbors and each pair of non-adjacent vertices have n_μ common neighbors. The Paley graph P_q is an srg$(q, \frac{q-1}{2}, \frac{q-5}{4}, \frac{q-1}{4})$ graph. Thus, the set of eigenvalues of $A(P_q)$ has only 3 distinct values listed as [27]

- $\lambda_1 = \frac{q-1}{2}$ with multiplicity 1,
- $\lambda_2 = \frac{-1+\sqrt{q}}{2}$ with multiplicity $\frac{q-1}{2}$, and
- $\lambda_3 = \frac{-1-\sqrt{q}}{2}$ with multiplicity $\frac{q-1}{2}$.

In fact, the multiplicity of the least eigne-value is a key to our sensing matrix construction in this paper.

III. Sensing Matrix Construction

Our design is based on the adjacency matrix of Paley graphs. Let q be a prime power of the form $q = 4a+1$, and let $A(P_q)$ be the adjacency matrix of the corresponding Paley graph. Since $A(P_q)$ is real-valued and symmetric, it has an eigen-decomposition of the form

$$A(P_q) = \mathbf{U}_{q\times q}\, \mathbf{D}_{q\times q}\, \mathbf{U}^{-1}_{q\times q}, \tag{5}$$

where $\mathbf{U}_{q\times q}$ is a unitary matrix whose columns are eigen-vectors of $A(P_q)$, and $\mathbf{D}_{q\times q}$ is a diagonal matrix that has the eigen-values on its diagonal.

Construction 1. *Let $\mathbf{u}_1$ be the unit-norm eigen-vector of the Paley adjacency matrix $A(P_q)$ associated with its largest eigen-value $\lambda_1 = \frac{q-1}{2}$, and let $\mathbf{u}_2, \ldots, \mathbf{u}_{\frac{q+1}{2}}$ be an orthonormal set of eigen-vectors of $A(P_q)$ corresponding to the eigen-value $\lambda_2 = \frac{-1+\sqrt{q}}{2}$ (second largest eigen-value). We define the sensing matrix by*

$$\mathbf{\Phi}_{(\frac{q+1}{2})\times q} = \mathbf{\Lambda}_{(\frac{q+1}{2})\times(\frac{q+1}{2})} \left[\mathbf{u}_1\ \mathbf{u}_2\ \ldots\ \mathbf{u}_{\frac{q+1}{2}}\right]^H, \tag{6}$$

where the diagonal matrix $\mathbf{\Lambda}$ is

$$\mathbf{\Lambda}_{(\frac{q+1}{2})\times(\frac{q+1}{2})} = \mathrm{diag}\Big(\sqrt{1-\tfrac{\lambda_1}{\lambda_3}}, \underbrace{\sqrt{1-\tfrac{\lambda_2}{\lambda_3}}, \ldots, \sqrt{1-\tfrac{\lambda_2}{\lambda_3}}}_{\frac{q-1}{2}\text{ times}}\Big). \tag{7}$$

(note that $\lambda_3 = \frac{-1-\sqrt{q}}{2} < 0$; hence, $1-\frac{\lambda_1}{\lambda_3}, 1-\frac{\lambda_2}{\lambda_3} > 0$)

Theorem 2. *For the matrix $\mathbf{\Phi}_{(\frac{q+1}{2})\times q}$ of Construction 1 we have that*

(i) the Gram matrix $\mathbf{\Phi}^H\mathbf{\Phi}$ is non-negative-valued,
(ii) the columns of $\mathbf{\Phi}$ have unit norm,
(iii) the coherence of $\mathbf{\Phi}$ is $\mu(\mathbf{\Phi}) = \frac{2}{1+\sqrt{q}}$, and
(iv) $\mathbf{\Phi}$ satisfies the RIP of order $k < \frac{3+\sqrt{q}}{2}$ with isometry constant $\delta_k \le \frac{2(k-1)}{1+\sqrt{q}}$.

Proof. Let us further define $\mathbf{u}_{\frac{q+3}{2}}, \ldots, \mathbf{u}_q$ to be an orthonormal set of eigen-vectors of $A(P_q)$ corresponding to the least eigen-value $\lambda_3 = \frac{-1-\sqrt{q}}{2}$. To proceed with the analysis, we introduce an auxiliary matrix $\widetilde{\mathbf{\Phi}}_{q\times q}$, which is an extension of $\mathbf{\Phi}_{(\frac{q+1}{2})\times q}$ to a square matrix by adding zeros:

$$\begin{aligned}\widetilde{\mathbf{\Phi}}_{q\times q} &= \begin{bmatrix}\mathbf{\Phi}\\ \mathbf{0}\end{bmatrix}_{q\times q}\\ &= \begin{bmatrix}\mathbf{\Lambda}_{(\frac{q+1}{2})\times(\frac{q+1}{2})} & \mathbf{0}\\ \mathbf{0} & \mathbf{0}\end{bmatrix}_{q\times q} [\mathbf{u}_1\ \mathbf{u}_2\ \ldots\ \mathbf{u}_q]^H. \end{aligned}\tag{8}$$

It is not difficult to verify that $\mathbf{\Phi}^H\mathbf{\Phi} = \widetilde{\mathbf{\Phi}}^H\widetilde{\mathbf{\Phi}}$, as the added zeros do not contribute in the Gram matrix. This enables us to write that

$$\begin{aligned}\mathbf{\Phi}^H\mathbf{\Phi} &= \underbrace{[\mathbf{u}_1\ \mathbf{u}_2\ \ldots\ \mathbf{u}_q]}_{\mathbf{U}} \begin{bmatrix}\mathbf{\Lambda} & \mathbf{0}\\ \mathbf{0} & \mathbf{0}\end{bmatrix}^2_{q\times q} [\mathbf{u}_1\ \mathbf{u}_2\ \ldots\ \mathbf{u}_q]^H\\ &= \mathbf{U}\,\mathrm{diag}\big(1-\tfrac{\lambda_1}{\lambda_3}, \underbrace{1-\tfrac{\lambda_2}{\lambda_3}, \ldots, 1-\tfrac{\lambda_2}{\lambda_3}}_{\frac{q-1}{2}\text{ times}}, \underbrace{0, \ldots, 0}_{\frac{q-1}{2}\text{ times}}\big)\,\mathbf{U}^H\\ &= \mathbf{U}\,\mathrm{diag}\big(1-\tfrac{\lambda_1}{\lambda_3}, \underbrace{1-\tfrac{\lambda_2}{\lambda_3}, \ldots, 1-\tfrac{\lambda_2}{\lambda_3}}_{\frac{q-1}{2}\text{ times}}, \underbrace{1-\tfrac{\lambda_3}{\lambda_3}, \ldots, 1-\tfrac{\lambda_3}{\lambda_3}}_{\frac{q-1}{2}\text{ times}}\big)\,\mathbf{U}^H\\ &= \mathbf{U}\,\mathbf{U}^H - \tfrac{1}{\lambda_3}\mathbf{U}\,\mathrm{diag}\big(\lambda_1, \underbrace{\lambda_2, \ldots, \lambda_2}_{\frac{q-1}{2}\text{ times}}, \underbrace{\lambda_3, \ldots, \lambda_3}_{\frac{q-1}{2}\text{ times}}\big)\,\mathbf{U}^H\\ &= \mathbf{I}_{q\times q} - \tfrac{1}{\lambda_3}A(P_q), \end{aligned}\tag{9}$$

where we invoked eigen-decomposition of $A(P_q)$ as in (5), and the fact that $\mathbf{U}$ is a unitary matrix.

Since $\lambda_3 < 0$ and $A(P_q)$ is a binary matrix, it is trivial to conclude (i) from (9). Furthermore, as there is no non-zero element on the diagonal of $A(P_q)$, (9) implies that the diagonal elements of $\mathbf{\Phi}^H\mathbf{\Phi}$ are all one. Thus, the columns of $\mathbf{\Phi}$ have unit norm and (ii) holds.

For matrices with unit-norm columns, the coherence in Definition 2 can be interpreted as the maximum modulus of the off-diagonal elements in the Gram matrix. For the introduced matrix $\mathbf{\Phi}$, this value coincides with the maximum element of $-\frac{1}{\lambda_3}A(P_q)$ which is clearly $-\frac{1}{\lambda_3} = \frac{2}{1+\sqrt{q}}$. This confirms (iii).

The claim in (iv) is a standard result obtained from the coherence bound using Gershgorin circle theorem: a matrix with unit-norm columns and coherence value μ satisfies the RIP of order $k < 1+\frac{1}{\mu}$ with isometry constant $\delta_k \le (k-1)\mu$ [7], [11]. □

Evaluating the Welch bound (3) for $m = \frac{q+1}{2}$ and $n = q$, we arrive at $\mu_{\text{Welch}} = \frac{1}{\sqrt{q+1}}$. This indicates that the coherence value in Theorem 2-(iii) is less than twice the Welch lower-bound, which is reasonable. Note that the Welch bound is valid for arbitrary complex-valued matrices while the introduced matrices are constrained to have non-negative-valued Gramians. The main drawback of the proposed design is that it does not provide flexibility in setting $\frac{n}{m}$ (aspect ratio of the sensing matrix), as it is almost fixed to 2.

IV. Simulations

In this section, we compare the performance of the new graph-based matrices with real-valued Gaussian random matrices and a design based on binary BCH codes [11]. The Gaussian ensembles are standard sensing matrices in the theory of compressed sensing and their performance in sparse vector recovery is generally regarded as ideal (optimal scaling). We also include BCH-based matrices as their Gramian is real-valued; however, the Gramian includes negative values. For the purpose of simulations, we set $q = 137$ which is a prime number and leads to a Paley graph of size 69×137. The coherence of this graph is $\mu_{\text{Paley}} = \frac{2}{1+\sqrt{69}} \approx 0.215$, which

guarantees RIP orders up to $k \leq 5$; this bound is sufficient to ensure stable recovery of only 2-sparse vectors. We use the same size (*i.e.*, 69×137) for generating Gaussian random matrices that are composed of zero-mean i.i.d. entries with normal distribution and variance $\frac{1}{69}$. To take full advantage of the randomness, we regenerate the Gaussian matrix for each realization of the sparse input vector. For a BCH-based matrix, we use the first 137 columns of a 63×256 bipolar matrix. The coherence of this matrix is $\mu_{\text{BCH}} = \frac{1}{7} \approx 0.143$. The comparison in this fashion is somewhat unfair against the BCH-based matrices as they are designed to take fewer samples for a higher input dimension ($n = 256$) and by removing the columns, the design remains unchanged. However, a better comparison was not permitted by the limitation that a generic BCH-based matrix is of size $(2^a - 1) \times 2^b$ for some integer a, b pairs, where $b = a + 1$ is not realizable.

In numerical results, we consider the recovery of sparse vectors both with and without measurement noise. Also for each realization of an n-dimensional k-sparse vector, we select the support (location of non-zero values) uniformly at random among all $\binom{n}{k}$ possibilities. Then, the k non-zero values are determined by k i.i.d. realizations of a standard normal distribution. For the recovery of a k-sparse vector $\mathbf{x}_{n\times 1}$ from compressed measurements $\mathbf{y}_{m\times 1} = \mathbf{\Phi}_{m\times n}\mathbf{x}_{n\times 1}$, we take advantage of the LASSO technique formulated by

$$\mathbf{x}_{n\times 1} = \arg\min_{\mathbf{s}_{n\times 1}} \left\|\mathbf{y} - \mathbf{\Phi}\mathbf{s}\right\|_2^2 + \tau\|\mathbf{s}\|_1,$$

where τ is optimized to yield the best average performance for each set of (m, n, k). The optimization over τ is performed by finding its optimal value for a number of known input vectors with the same sparsity and energy levels (oracle estimator) and using the average τ values for unknown inputs under the same sparsity and energy constraints.

Figure 2 shows the percentage of perfect recovery ($\text{SNR}_{\text{rec}} \geq 100$dB) when different sparsity orders k are considered. The percentages are evaluated based on 4000 trials for each matrix and each value of k. The results confirm superior performance of the Paley matrix compared to the other two. According to the curves, the samples from the Paley matrix can be used to perfectly recover k-sparse vectors with probability 1 for $k \leq 10$ and probability 0.9 for $k \leq 20$. Note that for $k = 20$, the probability of perfect reconstruction for Paley matrix is 90%, almost three times the probability for BCH-based matrices.

To study the stability of recovery, we investigate the performance under additive white Gaussian noise. For this purpose, we fix the sparsity order to $k = 20$ and vary the noise level (input SNR). For each of the matrix types, and each input SNR value, we perform the sampling/reconstruction procedure 1000 times and evaluate the average SNR of the reconstructed vectors. The results are depicted in Figure 3. While the three curves are very close at low SNRs, they separate at high SNRs. This implies that for a medium to high average quality in the reconstruction, we can tolerate higher noise levels when using the Paley matrix.

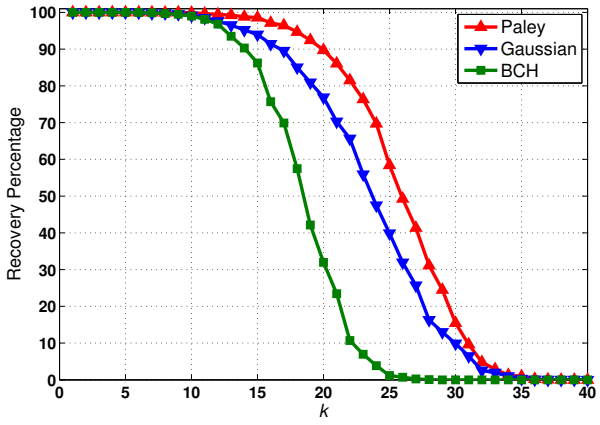

Fig. 2. The recovery percentage ($\text{SNR}_{\text{rec}} \geq 100$dB) for different sparsity values (k).

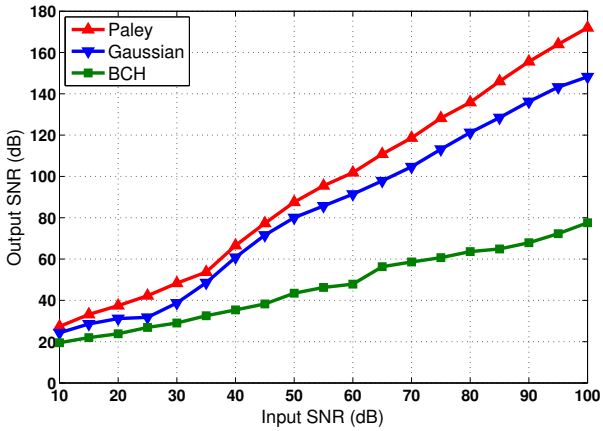

Fig. 3. The SNR of the reconstructed signal for 20-sparse signals when the compressed samples are accompanied with different noise powers.

V. Conclusion

In this paper, we introduced a technique to design $\frac{q+1}{2} \times q$ sensing matrices for prime powers q of the form $4a + 1$. The design is based on the eigen-decomposition of the adjacency matrix of Paley graphs and achieves coherence values no larger than twice the universal lower-bound of Welch. Due to the use of adjacency matrices, the Gramians of the constructed matrices are real-valued with no negative values. Numerical simulations show that the proposed matrices perform similar to and sometimes better than Gaussian random matrices of the same size when LASSO is employed. For instance, the range of sparsity orders up to which the recovery with probability 1 is provided is almost the same as the bounds for random matrices, which is considerably larger than the coherence bound. Furthermore, the recovery performance in the noisy setup confirms stability of the compressed samples against additive noise.

REFERENCES

[1] D. L. Donoho, "Compressed sensing," *IEEE Trans. Inform. Theory*, vol. 52, no. 4, pp. 1289–1306, Apr. 2006.

[2] E. J. Candés and M. B. Wakin, "An introduction to compressive sampling," *IEEE Sig. Proc. Magazine*, vol. 25, no. 2, pp. 21–30, Mar. 2008.

[3] D. L. Donoho and M. Elad, "Optimally sparse representation in general (nonorthogonal) dictionaries via ℓ_1 minimization," *Proc. Nat. Acad. Sci.*, vol. 100, no. 5, pp. 2197–2202, Mar. 2003.

[4] A. Cohen, W. Dahmen, and R. DeVore, "Compressed sensing and best k-term approximation," *J. Amer. Math. Soc.*, vol. 22, no. 1, pp. 211–231, 2009.

[5] E. J. Candés, "The restricted isometry property and its implications for compressed sensing," *Comptes Rendus Mathematique*, no. 9, pp. 589–592.

[6] R. Baraniuk, M. Davenport, R. DeVore, and M. Wakin, "A simple proof of the restricted isometry property for random matrices," *Constr. Approx.*, vol. 28, no. 3, pp. 253–263, Dec. 2008.

[7] R. A. DeVore, "Deterministic constructions of compressed sensing matrices," *J. of Complexity*, no. 4, pp. 918–925.

[8] S. Howard, S. Searle, and A. R. Calderbank, "Chirp sensing codes: Deterministic compressed sensing measurements for fast recovery," *Appl. and Comput. Harmonic Anal.*, vol. 26, no. 2, pp. 283–290, Mar. 2009.

[9] A. R. Calderbank, S. Howard, and S. Jafarpour, "Construction of a large class of deterministic sensing matrices that satisfy a statistical isometry property," *IEEE J. of Selected Topics in Sig. Proc.*, vol. 4, no. 2, pp. 358–374, Apr. 2010.

[10] S. D. Howard, A. R. Calderbank, and S. Searle, "A fast reconstruction algorithm for deterministic compressive sensing using second order Reed-Muller codes," in *Proc. of Conf. on Inform. Scie. and Sys. (CISS), 2008. CISS 2008. 42nd Annual Conference on*. IEEE, Mar. 19–21, 2008, pp. 11–15.

[11] A. Amini and F. Marvasti, "Deterministic construction of binary, bipolar and ternary compressed sensing matrices," *IEEE Trans. Inform. Theory*, vol. 57, no. 4, pp. 2360–2370, Apr. 2011.

[12] A. Amini, V. Montazerhodjat, and F. Marvasti, "Matrices with small coherence using p-ary block codes," *IEEE Trans. Sig. Proc.*, vol. 60, no. 1, pp. 172–181, Jan. 2012.

[13] M. F. Duarte, S. Jafarpour, and A. R. Calderbank, "Performance of the Delsarte-Goethals frame on clustered sparse vectors," *IEEE Trans. Sig. Proc.*, vol. 61, no. 8, pp. 1998–2008, Apr. 2013.

[14] M. M. Mohades, A. Mohades, and A. Tadaion, "A Reed-Solomon code based measurement matrix with small coherence," *IEEE Sig. Proc. Letters*, vol. 21, no. 7, pp. 839–843, Jul. 2014.

[15] S. Li, F. Gao, G. Ge, and S. Zhang, "Deterministic construction of compressed sensing matrices via algebraic curves," *IEEE Trans. Inform. Theory*, vol. 58, no. 8, pp. 5035–5041, Aug. 2012.

[16] S. Li and G. Ge, "Deterministic construction of sparse sensing matrices via finite geometry," *IEEE Trans. Sig. Proc.*, vol. 62, no. 11, pp. 2850–2859, Jun. 2014.

[17] N. Y. Yu, "New construction of a near-optimal partial Fourier codebook using the structure of binary m-sequences," in *Proc. of IEEE Int. Sym. on Inform. Theory (ISIT)*, Jul. 1–6, 2012, pp. 2436–2440.

[18] H. Zörlein and M. Bossert, "Coherence optimization and best complex antipodal spherical codes," *arXiv:1404.5889*, 2014.

[19] T. Strohmer and R. W. Heath, "Grassmannian frames with applications to coding and communication," *Appl. and Comp. Harm. Anal.*, vol. 14, no. 3, pp. 257–275, May 2003.

[20] J. Jasper, D. G. Mixon, and M. Fickus, "Kirkman equiangular tight frames and codes," *IEEE Trans. Inform. Theory*, vol. 60, no. 1, pp. 170–181, Jan. 2014.

[21] J. Bourgain, S. Dilworth, K. Ford, S. Konyagin, and D. Kutzarova, "Explicit constructions of RIP matrices and related problems," *Duke Math. J.*, vol. 159, no. 1, pp. 145–185, 2011.

[22] D. G. Mixon, "Explicit matrices with the restricted isometry property: Breaking the square-root bottleneck," *arXiv:1403.3427*, 2014.

[23] P. Indyk, "Explicit constructions for compressed sensing of sparse signals," in *Proc. of ACM-SIAM Symp. on Disc. Alg.*, Jan. 20–22, 2008, pp. 30–33.

[24] W. Xu and B. Hassibi, "Efficient compressive sensing with deterministic guarantees using expander graphs," in *Proc. Inform. Theory Workshop (ITW)*, Sep. 2–6, 2007, pp. 414–419.

[25] S. Jafarpour, W. Xu, B. Hassibi, and A. R. Calderbank, "Efficient and robust compressed sensing using optimized expander graphs," *IEEE Trans. Inform. Theory*, vol. 55, no. 9, pp. 4299–4308, Sep. 2009.

[26] A. S. Tehrani, A. G. Dimakis, and G. Caire, "Optimal deterministic compressed sensing matrices," in *Proc. of IEEE Int. Conf. on Speech and Sig.l Proc. (ICASSP)*, May 26–31, 2013, pp. 5895–5899.

[27] C. Godsil and G. Royle, *Algebraic Graph Theory*. Springer, 2004.